

FTIR Study of Adsorption and Surface Reactions of $\text{N}(\text{CH}_3)_3$ on TiO_2

Chen-Fu Lien, Yu-Feng Lin, Yi-Shiue Lin, Meng-Tso Chen, and Jong-Liang Lin*

Department of Chemistry, National Cheng Kung University, 1, Ta Hsueh Road, Tainan, Taiwan, Republic of China

Received: January 24, 2005; In Final Form: April 1, 2005

Fourier transform infrared spectroscopy has been employed to investigate the $\text{N}(\text{CH}_3)_3$ adsorption, thermal stability, and photochemical reactions on powdered TiO_2 . $\text{N}(\text{CH}_3)_3$ molecules are adsorbed on TiO_2 without dissociation at 35 °C and are completely desorbed from the surface at 300 °C in a vacuum. The CH_3 rocking frequencies of $\text{N}(\text{CH}_3)_3$ on TiO_2 are affected via the interaction between $\text{N}(\text{CH}_3)_3$ and TiO_2 surface OH groups. In the presence of O_2 , adsorbed $\text{N}(\text{CH}_3)_3$ decomposes thermally at 230 °C and photochemically under UV irradiation. In the latter case with comparative $^{16}\text{O}_2$ and $^{18}\text{O}_2$ studies, $\text{CO}_{2(\text{g})}$, $\text{NCO}_{(\text{a})}$, $\text{HCOO}_{(\text{a})}$, and surface species containing $\text{C}=\text{N}$ or NH_x functional groups are identified to be the photoreaction products or intermediates. In the presence of $^{18}\text{O}_2$, the main formate species formed is $\text{HC}^{16}\text{O}^{18}\text{O}_{(\text{a})}$. As H_2O is added to the photoreaction system, a larger percentage of adsorbed $\text{N}(\text{CH}_3)_3$ is consumed. However, in the presence of $^{18}\text{O}_2$ and H_2O , the amount of $\text{HC}^{16}\text{O}^{18}\text{O}_{(\text{a})}$ becomes relatively small, compared to $\text{HC}^{16}\text{O}^{16}\text{O}_{(\text{a})}$. A mechanism is invoked to explain these results. Furthermore, based on the comparison of isotopic oxygens in the formate products obtained from $\text{CH}_3\text{O}_{(\text{a})}$ photooxidation in $^{16}\text{O}_2$ and $^{18}\text{O}_2$, it is concluded that the $\text{N}(\text{CH}_3)_3$ photooxidation does not generate $\text{CH}_3\text{O}_{(\text{a})}$ in which the oxygen belongs to TiO_2 .

Introduction

Photoreactions of some nitrogen-containing organics catalyzed by semiconductors in solution phase have been investigated. Various reaction types were reported, depending on the molecular structures of reactants.^{1–6} For example, under irradiation, aniline and toluidine in ethanol with suspended ZnO and dissolved O_2 were transformed into the corresponding azocompounds;¹ imides were generated from *N*-acylamine reactions in the presence of oxygenated aqueous suspensions of TiO_2 ;² primary amines reacted to form secondary amines in aqueous solution containing a powdered mixture of TiO_2 and platinum black^{4,5} and to form *N*-alkylidene amines in the presence of suspended TiO_2 in acetonitrile.⁶ The semiconductor-catalyzed photoreactions were surface chemical processes; however, adsorption and surface reactions were not characterized.

TiO_2 , a semiconductor with a ~ 3.2 eV band gap, has often been used as a photocatalyst in solar energy conversion and degradation of molecules detrimental to the environment. Previously, Primet et al. used $\text{N}(\text{CH}_3)_3$ as a probe molecule to investigate acidic properties of TiO_2 and suggested that $\text{N}(\text{CH}_3)_3$ was adsorbed on the Lewis acid sites and some surface OH groups of anatase TiO_2 showed a protonic acidity.⁷ Boccuzzi et al. observed the thermal decomposition of adsorbed $\text{N}(\text{CH}_3)_3$ on TiO_2 at 473 K in O_2 atmosphere.⁸ To our knowledge, a more detailed study of interaction between $\text{N}(\text{CH}_3)_3$ and TiO_2 has not been reported. $\text{N}(\text{CH}_3)_3$ is moderately toxic by inhalation and is used in organic synthesis, manufacture of disinfectants, etc. In the present study, adsorption, thermal stability, and photoreactions of $\text{N}(\text{CH}_3)_3$ on powdered TiO_2 are examined by Fourier transform infrared spectroscopy in a gas–solid interaction system.

Experimental Section

The sample preparation of TiO_2 powder supported on a tungsten fine mesh ($\sim 6 \text{ cm}^2$) has been described previously.^{9,10} In brief, TiO_2 powder (Degussa P25, $\sim 50 \text{ m}^2/\text{g}$, anatase 70%, rutile 30%) was dispersed in water/acetone solution to form a uniform mixture that was then sprayed onto a tungsten mesh. After that, the TiO_2 sample was mounted inside the IR cell for simultaneous photochemistry and FTIR spectroscopy. The IR cell with two CaF_2 windows for IR transmission down to 1000 cm^{-1} was connected to a gas manifold that was pumped by a 60 L/s turbomolecular pump with a base pressure of $\sim 1 \times 10^{-7}$ Torr (1 Torr = 1.33×10^{-3} bar). The TiO_2 sample in the cell was heated to 450 °C under vacuum for 24 h by resistive heating. The temperature of the TiO_2 sample was measured by a K-type thermocouple spot-welded on the tungsten mesh. Before each run of the experiment, the TiO_2 sample was heated to 450 °C in a vacuum for 2 h. After heating, 10 Torr of O_2 was introduced into the cell as the sample was cooled to 70 °C. When the TiO_2 temperature reached 35 °C, the cell was evacuated for gas dosing. The TiO_2 surface after the above treatment still possessed residual isolated hydroxyl groups.¹¹ $^{16}\text{O}_2$ (99.998%, Matheson) and $^{18}\text{O}_2$ (99 atom %, Isotec) were used as received in compressed states. $\text{N}(\text{CH}_3)_3$ (45% aqueous solution, Merck-Schuchardt) was purified by several cycles of freeze–pump–thaw and introduced to the cell as the solution was cooled to ~ 3 °C to reduce the solubility of $\text{N}(\text{CH}_3)_3$ in the water and the evaporation of water molecules. Pressure was monitored with a Baratron capacitance manometer and an ion gauge. In the photochemistry study, both the UV and IR beams were set 45° to the normal of the TiO_2 sample. The UV light source used was a combination of a Hg arc lamp (Oriol Corp), a water filter, and a band-pass filter with a bandwidth of $\sim 100 \text{ nm}$ centered at 400 nm (Oriol 51670). The UV absorption of $\text{N}(\text{CH}_3)_3$ for the wavelengths used in the present study was negligible.¹² Infrared spectra were obtained with a 4 cm^{-1}

* Address correspondence to this author. E-mail: jonglin@mail.ncku.edu.tw. Phone: 886-6-275-7575, ext. 65326. Fax: 886-6-274-0552.

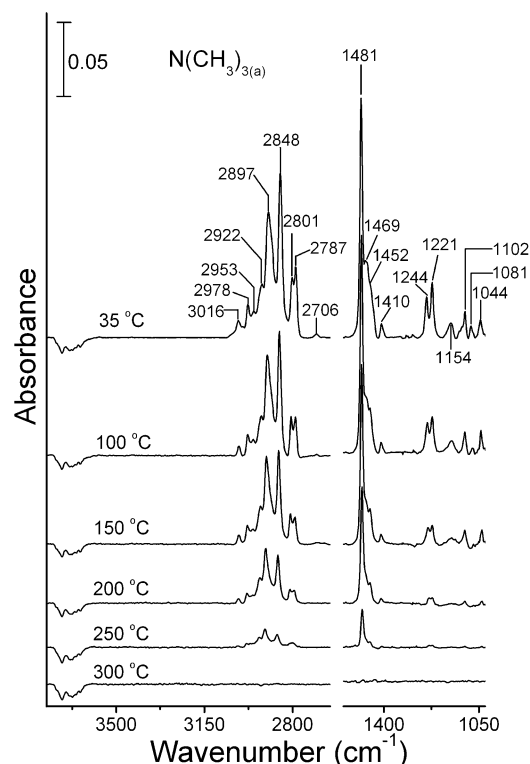


Figure 1. Infrared spectra of a TiO₂ surface exposed to ~0.4 Torr of N(CH₃)₃ and then evacuated at the indicated temperatures for 1 min. All the spectra were recorded at 35 °C with 50 scans.

resolution by a Bruker FTIR spectrometer with a MCT detector. The entire optical path was purged with CO₂-free dry air. The spectra presented here have been ratioed against a clean TiO₂ spectrum providing the metal-oxide background. In the study of photooxidation, the photoirradiation time count was started as the UV lamp was turned on. It took 40–50 s to reach full power. It was noted that in the present studies the infrared band frequencies obtained from different runs of experiments with the same conditions might vary by a few wavenumbers.

Results and Discussion

Adsorption of N(CH₃)₃ on TiO₂. Figure 1 shows the infrared spectra of a TiO₂ surface after being in contact with ~0.4 Torr of N(CH₃)₃ at 35 °C, followed by evacuation at the indicated temperatures for 1 min. All of the spectra in Figure 1 were taken at ~35 °C. Before analyzing the infrared spectra, it is worthy to note the CH₃ decoupling feature of N(CH₃)₃.^{13–15} In each CH₃ group of N(CH₃)₃, the C–H bond, trans to the lone-pair electrons of the N atom, has a lower stretching strength than that of the other two C–H bonds. The decoupling of the CH₃ into CH and CH₂ groups can be reasoned that the internal motion of the methyl group is so slow compared to the IR time scale that each of the C–H bonds is localized in one of the three potential minima. Another N(CH₃)₃ infrared absorption feature is that it shows relatively strong overtone and combination bands. In the 35 °C spectrum of Figure 1, infrared bands appear at 1044, 1081, 1102, 1154, 1221, 1244, 1410, 1452, 1469, 1481, 2706, 2787, 2801, 2848, 2897, 2922, 2953, 2978, and 3016 cm⁻¹. Table 1 compares the infrared frequencies of N(CH₃)₃ in the gas phase¹⁴ and on Ni(111),¹⁵ Pt(111),¹⁶ and TiO₂ of the present work. Our observed frequencies at 1044 ($\nu_{\text{as}}(\text{NC}_3)$), 1102 ($\rho'(\text{CH}_3)$), 1410 ($\delta_{\text{s}}(\text{CH}_3)$), 1469 ($\delta''_{\text{as}}(\text{CH}_3)$), 2953 ($\nu_{\text{s}}(\text{CH}_2)$), and 2978 cm⁻¹ ($\nu_{\text{as}}(\text{CH}_2)$) agree well with the corresponding fundamental modes of gaseous N(CH₃)₃, with a discrepancy ≤ 3

TABLE 1: Comparison of Infrared Frequencies (cm⁻¹) of N(CH₃)₃ in the Gas Phase and on Various Surfaces

gas phase (ref 14)	assignment ^a	Ni(111), 110 K (ref 15)	Pt(111), 85 K (ref 16)	TiO ₂ , 308 K (this work)
1043	$\nu_{\text{as}}(\text{NC}_3)$		1041	1044
				1081
1103	$\rho'(\text{CH}_3)$		1098	1102
1186	$\rho'(\text{CH}_3)$	1205	1187	1154
				1221
1275	$\rho''(\text{CH}_3)$		1271	1244
1409	$\delta_{\text{s}}(\text{CH}_3)$			1410
1459	$\delta'_{\text{as}}(\text{CH}_3)$	1463	1455	1452
1466	combination band			
1471	$\delta''_{\text{as}}(\text{CH}_3)$	1470		1469
1478	combination band			1481
2737	combination band			2706
2776	$\nu_{\text{s}}(\text{CH})$	2763	2731, 2768	2787
2824	overtone	2822		2801
2874	overtone	2873		2848
2898	combination band			2897
2940	combination band			2922
2953	$\nu_{\text{s}}(\text{CH}_2)$		2817, 2945	2953
2981	$\nu_{\text{as}}(\text{CH}_2)$		2973	2978
				3016

^a ν : stretching. δ : deformation. ρ : rocking.

cm⁻¹. This resemblance indicates the presence of N(CH₃)₃ on TiO₂. The 2787 cm⁻¹ ($\nu_{\text{s}}(\text{CH})$) band of the adsorbed N(CH₃)₃ is 11 cm⁻¹ higher than that of gaseous N(CH₃)₃. For the 1186 and 1275 cm⁻¹ CH₃ rocking bands of gaseous N(CH₃)₃, no closely matched bands are observed in the 35 °C spectrum of Figure 1, but at 1081, 1154, 1221, and 1244 cm⁻¹ instead. This implies either some of the N(CH₃)₃ molecules dissociate, forming new surface species responsible for the infrared bands, or the interaction between adsorbed N(CH₃)₃ and TiO₂ surface alters some of the infrared frequencies of the surface N(CH₃)₃. The TiO₂ surface used in this study possessed isolated OH groups, Ti⁴⁺ Lewis acid sites, and Ti³⁺ defect sites.^{17–19} In the theoretical calculations of NH₃ adsorption on rutile TiO₂, it has been shown that NH₃ can be bound to surface OH via hydrogen bonding and to Ti⁴⁺ via Lewis acid–base interaction.²⁰ Similar interactions may apply to the adsorbed N(CH₃)₃ on powdered TiO₂. Furthermore, previous studies of hydrogen bonding interactions between hydrogen halides (HF, HCl, HBr, and HI) and N(CH₃)₃ showed that the CH₃ rocking modes of N(CH₃)₃ in N(CH₃)₃–hydrogen halide complexes were indeed significantly affected, compared to those of free N(CH₃)₃ molecules.^{21–23} For example, the 1269 cm⁻¹ rocking band of free N(CH₃)₃ is shifted to 1215 cm⁻¹ after forming an acid–base complex with HF in Ar matrix; the N(CH₃)₃–HCl complex absorbs at 1004, 1197, and 1220 cm⁻¹, in contrast to the 1043, 1186, and 1275 cm⁻¹ of free N(CH₃)₃ molecules. Similarly, the N(CH₃)₃–HBr complex absorbs at 1000, 1196, and 1225 cm⁻¹ and the N(CH₃)₃–HI complex absorbs at 1002, 1206, and 1250 cm⁻¹. In the 35 °C spectrum of Figure 1, the negative bands in the 3500–3800 cm⁻¹ region represent the decrease of isolated OH groups on TiO₂ after N(CH₃)₃ adsorption, indicating the presence of interaction between the surface OH groups and adsorbed N(CH₃)₃ and corroborating the lower CH₃ rocking frequencies of N(CH₃)₃ on TiO₂. Although the interaction between adsorbed N(CH₃)₃ and surface OH groups is evidenced, the interaction between adsorbed N(CH₃)₃ and Ti⁴⁺ cannot be ruled out.

From the temperature-dependent spectra shown in Figure 1, the band intensities of adsorbed N(CH₃)₃ decrease upon heating to 100 °C and disappear at a temperature of 300 °C in a vacuum, without forming new bands. This result suggests that N(CH₃)₃ is molecularly adsorbed on the surface at 35 °C and totally

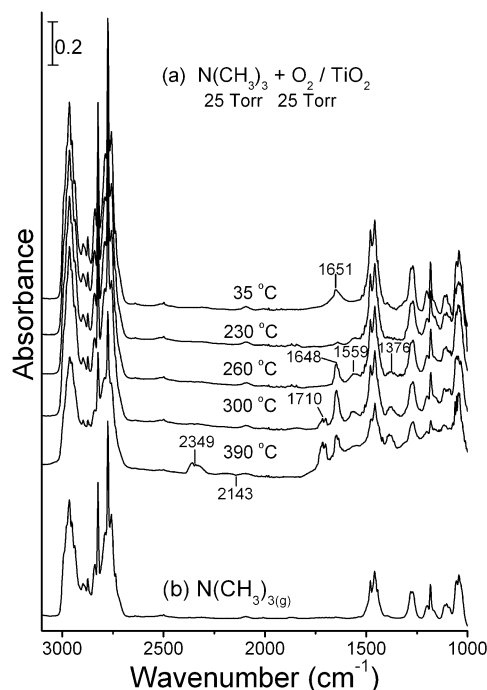


Figure 2. (a) Development of infrared spectra of a mixture of ~ 25 Torr of $\text{N}(\text{CH}_3)_3$ and ~ 25 Torr of O_2 over a TiO_2 surface heated at a rate of 2°C/s ; (b) infrared spectrum of gaseous $\text{N}(\text{CH}_3)_3$. All the spectra in part a were recorded at the indicated temperatures with 5 scans.

desorbed without dissociation after heating to 300°C . There is other indirect evidence that supports the molecular adsorption of $\text{N}(\text{CH}_3)_3$ on TiO_2 . If the C–N bonds of $\text{N}(\text{CH}_3)_3$ dissociate, adsorbed CH_3O groups are expected to be generated, because the dissociative CH_3I adsorption, via C–I bond scission, on TiO_2 has shown the formation of adsorbed CH_3O .²⁴ CH_3O on TiO_2 absorbs at ~ 1045 , 1125 , 2825 , and 2925 cm^{-1} .²⁵ If the C–H bonds of $\text{N}(\text{CH}_3)_3$ dissociate, surface OH absorptions between 3500 and 3800 cm^{-1} and/or C=N absorptions between 1580 and 1690 cm^{-1} are expected to be enhanced.²⁶ But this is not the case in the present study.

Thermal Reactions of $\text{N}(\text{CH}_3)_3$ on TiO_2 in the Presence of O_2 . Figure 2a shows the spectra taken at the indicated temperatures for a mixture of ~ 25 Torr of $\text{N}(\text{CH}_3)_3$ and ~ 25 Torr of O_2 initially in contact with a TiO_2 surface at 35°C in a close cell. The surface temperature was increased linearly from 35°C to 400°C at a rate of 2°C/s . A gaseous $\text{N}(\text{CH}_3)_3$ spectrum is also shown in Figure 2b for comparison. The 35°C spectrum of Figure 2a can be attributed to the absorptions of $\text{N}(\text{CH}_3)_3$ present on TiO_2 and in the gas phase. However, the broad peak at 1651 cm^{-1} is probably due to the combination mode (1640 cm^{-1}) of $\text{N}(\text{CH}_3)_3$ ¹⁴ overlapped with the bending mode of adsorbed H_2O , which is introduced to the cell at such a high $\text{N}(\text{CH}_3)_3$ dosage. As the temperature is increased to 230°C , this band becomes smaller because of the partial desorption of adsorbed $\text{N}(\text{CH}_3)_3$ and H_2O . Six new bands appear at 1376 , 1559 , 1648 , 1710 , 2143 , and 2349 cm^{-1} during the heating process up to 400°C . It has been reported that $\text{HCOO}_{(\text{a})}$ produced from HCOOH dissociative adsorption on TiO_2 has two strong absorption bands at 1370 and 1555 cm^{-1} .²⁷ Formamide also dissociates on TiO_2 , producing adsorbed $\eta^2(\text{N},\text{O})\text{-HCONH}$ with two strong bands at 1355 and 1568 cm^{-1} .²⁸ Additionally, in the investigation of the NO_2/TiO_2 adsorption system heated at 375°C , three bands at 1360 , 1440 (relatively small), and 1550 cm^{-1} have been measured. The 1440 and 1550 cm^{-1} bands are suggested to be due to a nitro–nitrito complex, i.e., attached to the Ti^{4+} ion by N and O atoms simultaneously.²⁹

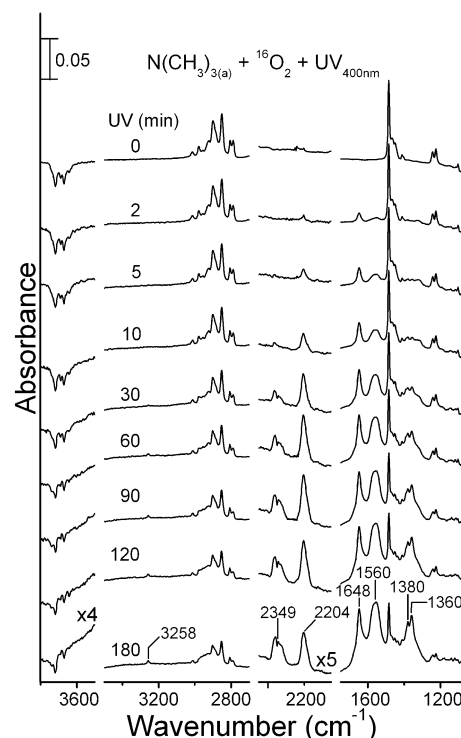


Figure 3. Infrared spectra taken after the indicated times during UV irradiation of $\text{N}(\text{CH}_3)_3$ adsorbed on TiO_2 initially in 10 Torr of $^{16}\text{O}_2$ in a closed cell. All the spectra were recorded with 5 scans. All the traces in $2050\text{--}2450$ and $3500\text{--}3800\text{ cm}^{-1}$ are multiplied by a factor of 5 and 4, respectively.

Therefore, the 1376 and 1559 cm^{-1} bands observed in Figure 2 are likely due to HCOO , HCONH , and/or a nitro–nitrito complex on the surface. The 1648 and 1710 cm^{-1} bands are assigned to C=N and C=O stretching vibrations.²⁶ The carbonyl stretching modes of formic acid²⁷ and formamide²⁸ on TiO_2 have been detected at $\sim 1680\text{ cm}^{-1}$. Because of not enough evidence, the responsible species for the 1648 and 1710 cm^{-1} bands are not determined. The 2143 and 2349 cm^{-1} bands are due to CO and CO_2 formed in the gas phase, respectively. The 1559 cm^{-1} band appears at 230°C , revealing that $\text{N}(\text{CH}_3)_3$ dissociates on TiO_2 at this temperature. A similar thermal experiment was also carried out, but without O_2 . It was found that, except for the infrared bands belonging to $\text{N}(\text{CH}_3)_3$, no new bands were detected.

Oxidation of $\text{N}(\text{CH}_3)_3$ on TiO_2 under Photoirradiation in the Presence of O_2 . Figure 3 shows the infrared spectra taken after the indicated times during 400 nm photoirradiation of a TiO_2 surface covered with $\text{N}(\text{CH}_3)_3$ initially in 10 Torr of $^{16}\text{O}_2$. Inspecting the change of the spectra with photoirradiation time, it is found that the amount of adsorbed $\text{N}(\text{CH}_3)_3$ decreases and that new bands appear, indicating photodecomposition of $\text{N}(\text{CH}_3)_3$ and formation of new species. The new bands resulting from $\text{N}(\text{CH}_3)_3$ photodecomposition appear at 1360 , 1380 , 1560 , 1648 , 2204 , 2349 , and 3258 cm^{-1} after 180 min of photoirradiation. The 1560 and 1648 cm^{-1} bands appear in the early illumination stage, ~ 2 min. Among the observed new bands, the 2349 cm^{-1} band is directly attributed to gaseous CO_2 and its size increases continuously with photoirradiation. To correctly assign the other observed bands, photooxidation of $\text{N}(\text{CH}_3)_3$ on TiO_2 in $^{18}\text{O}_2$ was investigated as well. Figure 4 shows the infrared spectra taken after the indicated times during 400 nm of photoirradiation of a TiO_2 surface covered with $\text{N}(\text{CH}_3)_3$ in 10 Torr of $^{18}\text{O}_2$. In the infrared analysis for Figures 3 and 4, the band assignments are based on characteristic frequencies

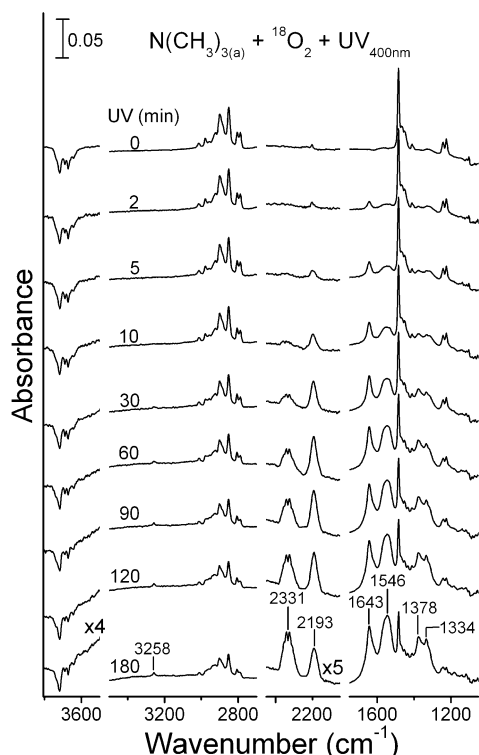


Figure 4. Infrared spectra taken after the indicated times during UV irradiation of $\text{N}(\text{CH}_3)_3$ adsorbed on TiO_2 initially in 10 Torr of $^{18}\text{O}_2$ in a closed cell. All the spectra were recorded with 5 scans. All the traces in 2050–2450 and 3500–3800 cm^{-1} are multiplied by a factor of 5 and 4, respectively.

of functional groups and shifts in frequency of oxygen-containing species.^{26,30} Compared to the bands found in the $^{16}\text{O}_2$ case, any red-shifted bands in Figure 4 suggest that the species responsible for them possess ^{18}O . As an example, the 2349 cm^{-1} $\text{C}^{16}\text{O}_{2(\text{g})}$ band in the $^{16}\text{O}_2$ case is red-shifted to 2331 cm^{-1} in the 180 min spectrum of Figure 4, which is attributed to $\text{C}^{18}\text{O}_{2(\text{g})}$. Other red-shifted bands with a frequency difference larger than 10 cm^{-1} include the 1334 cm^{-1} shifted from 1360 cm^{-1} , 1546 cm^{-1} from 1560 cm^{-1} , and 2193 cm^{-1} from 2204 cm^{-1} . The 1378 and 1643 cm^{-1} bands are shifted, to a smaller extent, from 1380 and 1648 cm^{-1} , respectively. The band at 3258 cm^{-1} does not change in frequency and is assigned to the NH_x stretching mode. The 1643 cm^{-1} band belongs to the stretching vibration of the $\text{C}=\text{O}$ or $\text{C}=\text{N}$ functional group. However, the former functional group seems unlikely, because $\text{C}=\text{C}^{18}\text{O}$ stretching vibrations of organic compounds are expected to be about 25 cm^{-1} lower than $\text{C}=\text{C}^{16}\text{O}$ stretching vibrations.²⁶ The 2204 cm^{-1} band observed in Figure 3 is attributed to isocyanate species, $\text{NCO}_{(\text{a})}$. In the recent studies of photooxidation of CH_3CN on TiO_2 in O_2 , a similar band has been observed.^{31,32} The shift of the band at 2204 cm^{-1} in $^{16}\text{O}_2$ to 2193 cm^{-1} in $^{18}\text{O}_2$ is consistent with the CN frequency of $\text{NC}^{16}\text{O}_{(\text{a})}$ being higher than that of $\text{NC}^{18}\text{O}_{(\text{a})}$ on TiO_2 by a ~ 10 cm^{-1} .³² On TiO_2 , $\text{NCO}_{(\text{a})}$ formation has been reported first from the decomposition of isocyanic acid at 25 $^\circ\text{C}$.³³ The two strong bands at 1360 and 1560 cm^{-1} observed in the $^{16}\text{O}_2$ case are shifted to lower frequencies in the $^{18}\text{O}_2$ case by 26 and 14 cm^{-1} , respectively. The 1360 and 1560 cm^{-1} bands are assigned to $-\text{COO}-$ symmetric and antisymmetric stretching of $\text{HCOO}_{(\text{a})}$, with supports from the previous observation of similar frequencies of $\text{HCOO}_{(\text{a})}$ produced by the dissociative adsorption of formic acid and formaldehyde on TiO_2 .^{27,34,35} In the oxygen isotopic study for HCOONa , the symmetric stretching of $-\text{C}^{16}\text{O}^{16}\text{O}-$, $-\text{C}^{16}\text{O}^{18}\text{O}-$, and $-\text{C}^{18}\text{O}^{18}\text{O}-$ absorb at 1340, 1315, and 1297 cm^{-1} ,

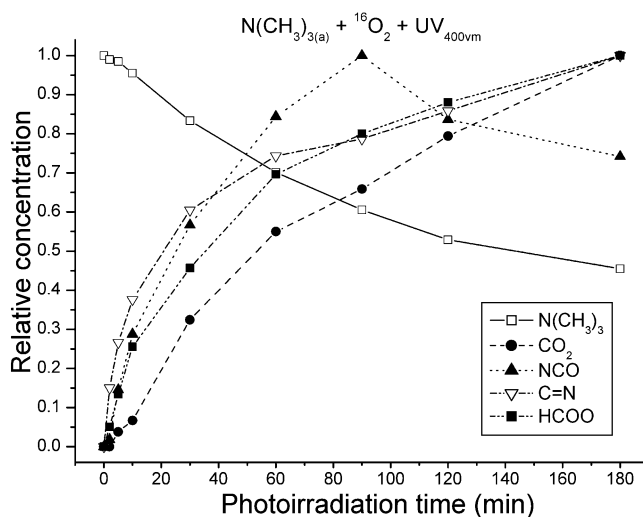


Figure 5. Relative concentrations of the major species detected in the photodecomposition of $\text{N}(\text{CH}_3)_3$ on TiO_2 in $^{16}\text{O}_2$ as a function of photoirradiation time. The maximum amount for each species during the irradiation process is scaled to 1.

respectively. On the other hand, the antisymmetric stretching of $-\text{C}^{18}\text{O}^{16}\text{O}-$ and $-\text{C}^{18}\text{O}^{18}\text{O}-$ absorb at 1607 and 1587 cm^{-1} , respectively.³⁶ The observed frequency shifts in Figures 3 and 4 for symmetric and antisymmetric stretching of formate on TiO_2 are consistent with the case of HCOONa . In addition, the 1380 cm^{-1} band in Figure 3 and the 1378 cm^{-1} band in Figure 4 are assigned to the $\text{C}-\text{H}$ deformation of formate on TiO_2 .³⁵ This comparative result of $^{16}\text{O}_2$ and $^{18}\text{O}_2$ also indicates the incorporation of O_2 in the formation of $\text{HCOO}_{(\text{a})}$ and $\text{NCO}_{(\text{a})}$ from $\text{N}(\text{CH}_3)_3$ photodecomposition on TiO_2 .

Figure 5 shows the relative concentrations of $\text{N}(\text{CH}_3)_3$ and its photodecomposition products of $\text{CO}_{2(\text{g})}$, $\text{NCO}_{(\text{a})}$, $\text{HCOO}_{(\text{a})}$, and the adsorbed species containing the $\text{C}=\text{N}$ group as a function of photoirradiation time for Figure 3. The $\text{N}(\text{CH}_3)_3$ decreases continuously with increasing irradiation time in contrast to the monotonically increased $\text{CO}_{2(\text{g})}$, $\text{HCOO}_{(\text{a})}$, and $\text{C}=\text{N}$. $\text{NCO}_{(\text{a})}$ increases to a maximum at 90 min and then decreases. In addition, 50% of the OH negative band area that is due to initial $\text{N}(\text{CH}_3)_3$ adsorption is restored after 180 min of photoirradiation, as shown in Figure 3.

Oxidation of $\text{N}(\text{CH}_3)_3$ on TiO_2 under Photoirradiation in the Presence of H_2O and O_2 . Figure 6 shows the infrared spectra taken after the indicated times during 400 nm of photoirradiation of a TiO_2 surface covered with $\text{N}(\text{CH}_3)_3$ and H_2^{16}O in 10 Torr of $^{16}\text{O}_2$. The TiO_2 surface subject to photoirradiation was prepared by adsorption of $\text{N}(\text{CH}_3)_3$, followed by exposure of H_2O vapor of ~ 0.4 Torr and evacuation at 35 $^\circ\text{C}$. In the 0-min spectrum, the infrared band of adsorbed H_2O is located at 1624 cm^{-1} . Similar to the case without H_2O , $\text{HCOO}_{(\text{a})}$ (1360, 1381, and 1566 cm^{-1}), $\text{NCO}_{(\text{a})}$ (2204 cm^{-1}), $\text{CO}_{2(\text{g})}$ (2349 cm^{-1}), and a species containing the $\text{C}=\text{N}$ group (1645 cm^{-1}) are generated upon photoirradiation. However, there are several different aspects. First, a band at 1173 cm^{-1} appears. Second, $\text{NCO}_{(\text{a})}$ increases to a maximum at 60 min and then declines. Third, a larger percentage of adsorbed $\text{N}(\text{CH}_3)_3$ is consumed in the presence of H_2O , i.e., 85% after 180 min of photoirradiation as compared to the 50% without H_2O in Figure 3. The larger percentage of consumption of $\text{N}(\text{CH}_3)_3$ in the presence of H_2O and O_2 may result from an increase of reactive initiation species for $\text{N}(\text{CH}_3)_3$ decomposition, such as O_2^- , hole, or OH^\bullet , or acceleration of consumption of the surface intermediates. In the former case, the recent chemiluminescence study has shown that the steady-state O_2^-

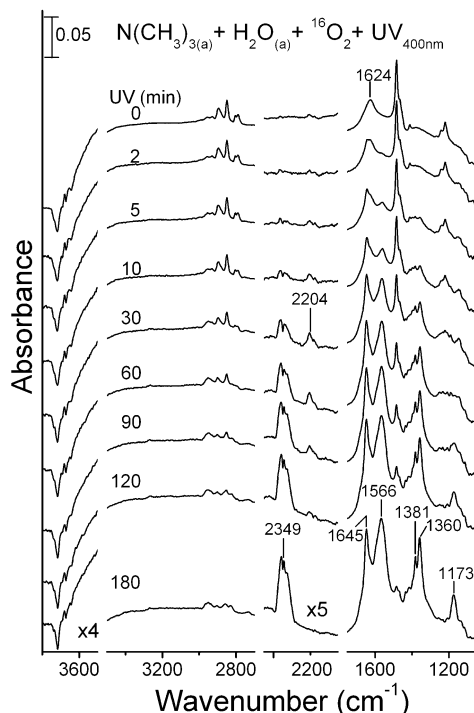


Figure 6. Infrared spectra taken after the indicated times during UV irradiation of a TiO_2 surface covered with $\text{N}(\text{CH}_3)_3$ and H_2O initially in 10 Torr of $^{16}\text{O}_2$ in a closed cell. All the spectra were recorded with 5 scans. All the traces in 2050–2450 and 3500–3800 cm^{-1} are multiplied by a factor of 5 and 4, respectively.

concentration produced for the TiO_2 – H_2O –air system under UV illumination is twice that for the TiO_2 –air system.³⁷ O_2^- is a possible initiation species for $\text{N}(\text{CH}_3)_3$ decomposition. Besides, O_2^- originates from photoelectron capture of O_2 , therefore the lifetime of holes can increase because of the retardation of electron–hole pair recombination, inducing more consumption of $\text{N}(\text{CH}_3)_3$ on TiO_2 . Furthermore, it is believed that photoholes can react with surface H_2O to form OH^\bullet radicals. If OH^\bullet is the active species, the presence of H_2O is expected to cause more $\text{N}(\text{CH}_3)_3$ molecules to decompose. In Figure 6, the 1168 cm^{-1} band falls in the absorption range of the C–N or C–N–C stretching vibration.²⁶ This peak cannot be assigned to NO, NO_2 , or NO_3 species on TiO_2 , because the infrared studies of adsorption of NO and NO_2 on TiO_2 have shown no bands at ~ 1170 cm^{-1} . NO on TiO_2 absorbs at ~ 1900 cm^{-1} .³⁸ Adsorption of NO_2 on TiO_2 generates surface NO_2 and NO_3 species with infrared absorptions between 1220 and 1640 cm^{-1} .²⁹ In addition, no band near 1170 cm^{-1} has been observed in the study of photooxidation of NH_3 on TiO_2 in O_2 .³⁹ Photoirradiation of $\text{N}(\text{CH}_3)_3$ on TiO_2 in the presence of H_2O only, without O_2 , was also investigated, but no infrared bands other than those of $\text{N}(\text{CH}_3)_3$ were observed during the irradiation.

Figure 7 shows the infrared spectra taken after the indicated times during 400 nm of photoirradiation of a TiO_2 surface covered with $\text{N}(\text{CH}_3)_3$ and H_2^{16}O in $^{18}\text{O}_2$. In this experiment, it is expected that the same species as those observed in Figure 6 are formed, but H_2O participation in the photoproduct formation is able to be studied. Most interestingly in Figure 7, the formate absorbs at 1356 and 1565 cm^{-1} with a small shoulder at 1332 cm^{-1} . This result indicates that most of the formate molecules generated in the presence of H_2^{16}O and $^{18}\text{O}_2$ possess two ^{16}O atoms, in contrast to the case in the presence of $^{18}\text{O}_2$ only, as shown in Figure 4. H_2O indeed involves in the formation of $\text{HCOO}_{(\text{a})}$ in the photodecomposition of $\text{N}(\text{CH}_3)_3$ on TiO_2 .

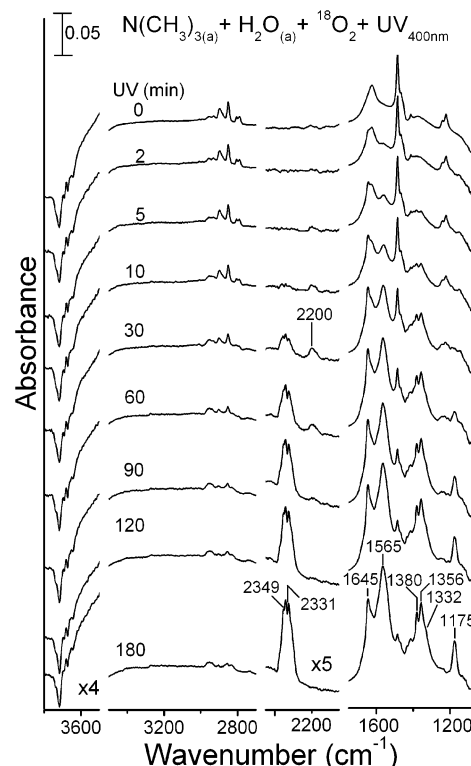


Figure 7. Infrared spectra taken after the indicated times during UV irradiation of a TiO_2 surface covered with $\text{N}(\text{CH}_3)_3$ and H_2O initially in 10 Torr of $^{18}\text{O}_2$ in a closed cell. All the spectra were recorded with 5 scans. All the traces in 2050–2450 and 3500–3800 cm^{-1} are multiplied by a factor of 5 and 4, respectively.

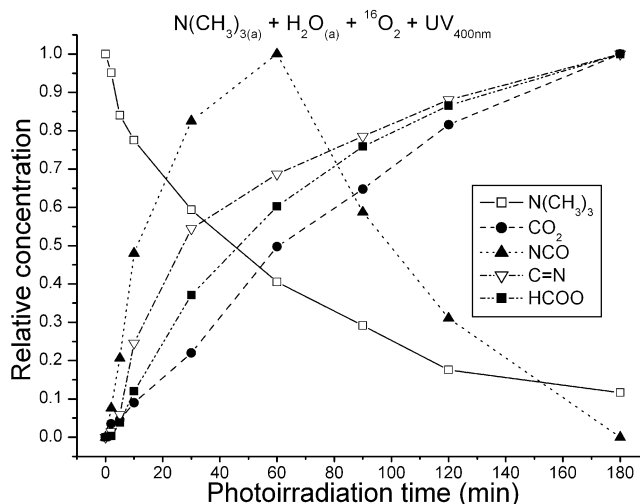
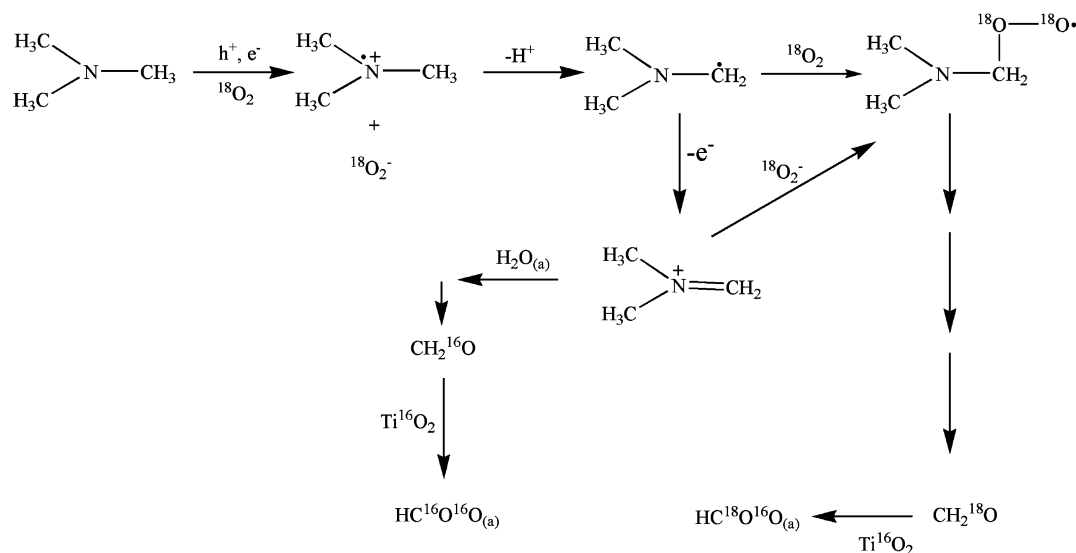


Figure 8. Relative concentrations of the major species detected in the photodecomposition of $\text{N}(\text{CH}_3)_3$ on TiO_2 in the presence of adsorbed H_2O and gaseous $^{16}\text{O}_2$ as a function of photoirradiation time. The maximum amount for each species during the irradiation process is scaled to 1.

Figure 8 shows the relative concentrations of $\text{N}(\text{CH}_3)_3$ and its photodecomposition products of $\text{CO}_{2(\text{g})}$, $\text{NCO}_{(\text{a})}$, $\text{HCOO}_{(\text{a})}$, and the adsorbed species containing the C=N group as a function of photoirradiation time for Figure 6. In comparison of Figures 5 and 8, it is found that a larger percentage of adsorbed $\text{N}(\text{CH}_3)_3$ is consumed after 180 min of photoirradiation in the presence of adsorbed H_2O . As observed in the 0-min spectra of Figures 3 and 6, the areas of the isolated OH negative bands are approximately the same. Using the same preparation process for a clean TiO_2 surface prior to $\text{N}(\text{CH}_3)_3$ adsorption, which would produce similar surface OH groups, the comparable

SCHEME 1



negative OH band areas suggest that the amounts of isolated surface OH groups on TiO₂ before N(CH₃)₃ photodecomposition are comparable for Figures 3 and 6. Therefore the difference in photoreactivity of N(CH₃)_{3(a)} in the presence of H₂O_(a) cannot be ascribed to the isolated OH groups. In the present study, the surface temperatures were raised to approximately 43 °C during photoirradiation experiments of N(CH₃)₃ on TiO₂. Therefore, thermal control experiments were carried out with the same conditions as those of the photoexperiments, but holding the TiO₂ surface at the corresponding temperatures without photon exposure. No decomposition of N(CH₃)₃ in these thermal experiments was observed.

Photooxidation of organic molecules catalyzed by TiO₂ is often suggested to be initiated by holes (or their trapped forms),

OH[•], and/or anionic oxygens, such as O₂⁻. As N(CH₃)₃ molecules are attacked by these reactive species, (CH₃)₂N-CH₂[•] radicals are likely to be formed.¹⁻⁶ One of the reaction routes for (CH₃)₂N-CH₂[•] is its recombination with O₂. This process is the origin for NCO_(a) and HCOO_(a) formation in the N(CH₃)₃ photodecomposition on TiO₂ in O₂. The formation of the intermediate with the C=N functional group can be ascribed to dehydrogenation and N-C bond scission of N(CH₃)₃. In fact, it has been reported that two 2-aminobutane (CH₃(H)C(NH₂)-C₂H₅) molecules recombine to form C₂H₅(CH₃)C=NC(H)-(CH₃)C₂H₅ in anhydrous acetonitrile with suspended TiO₂ powders upon photoirradiation.⁶ Although in the present study the N-C bonds break in the N(CH₃)₃ photodecomposition mediated by TiO₂, no CH₃O_(a) (with infrared absorptions at ~2825 and 2925 cm⁻¹ for CH₃ stretching vibrations and between 1000 and 1200 cm⁻¹ for C-O stretching vibrations)²⁵ formation is observed. However, CH₃O_(a) may be a transient species formed in the N(CH₃)₃ photooxidation on TiO₂, i.e., it decomposes immediately after it is generated. This point has been clarified by performing a comparative study of CH₃O_(a) photooxidation, forming adsorbed formate groups, in ¹⁶O₂ and ¹⁸O₂, as shown in Figure 9. In Figure 9a, CH₃¹⁶O_(a) in ¹⁶O₂ is photooxidized to form H₂¹⁶O_(a) (1625 cm⁻¹) and HC¹⁶O¹⁶O_(a) (1360 and 1560 cm⁻¹ for -COO- stretching vibrations). In the presence of ¹⁸O₂ as shown in Figure 9b, new peaks formed at 1335 and 1546 cm⁻¹ are attributed to HC¹⁶O¹⁸O_(a), but the main formate species is HC¹⁶O¹⁶O_(a). Compared to the N(CH₃)₃ photodecomposition in ¹⁶O₂ and ¹⁸O₂ (Figures 3 and 4), HC¹⁶O¹⁸O is the dominant form for the latter case. Therefore, it is concluded that, in the photodecomposition of N(CH₃)₃ on TiO₂ in O₂, CH₃O_(a) is unlikely to be the main reaction intermediate for HCOO_(a) formation. Besides, by invoking previously proposed reaction steps of amine oxidation,^{3,40-42} the mechanism in Scheme 1 is suggested to explain the observed isotopic form of formate species in the presence of O₂ and/or H₂O. In the photodecomposition of N(CH₃)₃ on TiO₂, it must involve multiple bond-forming and bond-breaking steps, i.e., the photodecomposition proceeds via multiple elementary reactions in order to form oxygenated compounds such as HCOO_(a), NCO_(a), etc. There are very likely other reaction intermediates not detected in the present study. Further studies are necessary for understanding a more complete N(CH₃)₃ photodecomposition process. It is interesting to make a com-

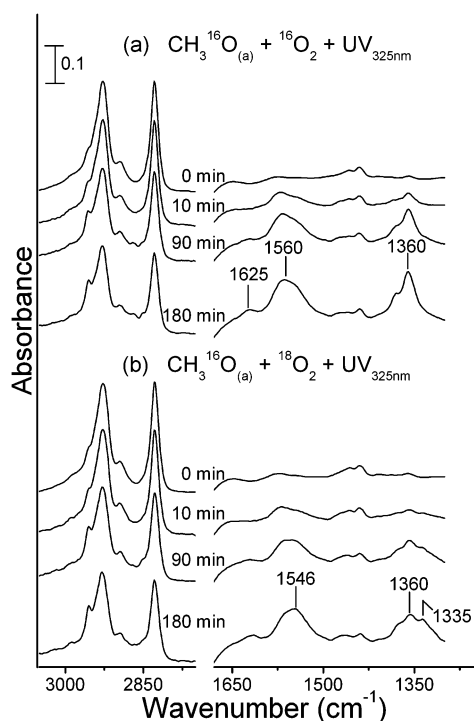


Figure 9. Infrared spectra taken after the indicated times during UV irradiation of a TiO₂ surface covered with CH₃O in 10 Torr of ¹⁶O₂ (a) and ¹⁸O₂ (b). The adsorbed CH₃O was prepared by CH₃OH adsorption on TiO₂ at 35 °C, followed by brief annealing to ~250 °C in a vacuum.

parison between the previous study of $\text{N}(\text{C}_2\text{H}_5)_3$ on TiO_2 and present study of $\text{N}(\text{CH}_3)_3$.⁴³ Because of the shifted CH_3 rocking frequencies of $\text{N}(\text{CH}_3)_3$ on TiO_2 , the interaction between the surface OH and adsorbed $\text{N}(\text{CH}_3)_3$ is clearly manifested. $\text{N}(\text{CH}_3)_3$ and $\text{N}(\text{C}_2\text{H}_5)_3$ thermally decompose on TiO_2 at a temperature higher than 200 °C in the presence of O_2 . Photo-oxidation of both $\text{N}(\text{CH}_3)_3$ and $\text{N}(\text{C}_2\text{H}_5)_3$ on TiO_2 in O_2 generates $\text{NCO}_{(\text{a})}$, $\text{HCOO}_{(\text{a})}$, and $\text{CO}_{2(\text{g})}$. $\text{H}_2\text{O}_{(\text{a})}$ and $\text{CH}_3\text{COO}_{(\text{a})}$ are also observed as photoproducts in the case of $\text{N}(\text{C}_2\text{H}_5)_3$. As suggested in the present study, $\text{CH}_3\text{COO}_{(\text{a})}$ may not be derived from direct C–N bond scission of $\text{N}(\text{C}_2\text{H}_5)_3$. The present $\text{N}(\text{CH}_3)_3$ study also shows that the effect of H_2O addition in the photoreaction of $\text{N}(\text{CH}_3)_3$ in O_2 is not due to surface OH groups.

Conclusions

On TiO_2 , $\text{N}(\text{CH}_3)_3$ molecules can be bound to surface OH groups and Lewis acid Ti^{4+} ions. The adsorbed $\text{N}(\text{CH}_3)_3$ molecules can be removed from the surface without thermal decomposition after heating to 300 °C in a vacuum. In the presence of O_2 , $\text{N}(\text{CH}_3)_3$ decomposes thermally at 230 °C. With photoirradiation in the presence of O_2 , the adsorbed $\text{N}(\text{CH}_3)_3$ decomposes and forms $\text{CO}_{2(\text{g})}$, $\text{NCO}_{(\text{a})}$, $\text{HCOO}_{(\text{a})}$, and surface species containing C=N or NH_x groups. $\text{CH}_3\text{O}_{(\text{a})}$ is unlikely to be the reaction intermediate for the $\text{HCOO}_{(\text{a})}$ formation. O_2 participates in the $\text{NCO}_{(\text{a})}$ and $\text{HCOO}_{(\text{a})}$ formation, i.e., incorporates its O into $\text{NCO}_{(\text{a})}$ and $\text{HCOO}_{(\text{a})}$. Upon photoirradiation of $\text{N}(\text{CH}_3)_3$ on TiO_2 in the presence of H_2O and O_2 , a larger percentage of $\text{N}(\text{CH}_3)_3$ is consumed, compared to the case with only O_2 . H_2O also plays a role in the $\text{HCOO}_{(\text{a})}$ formation, as suggested by using $^{18}\text{O}_2$.

Acknowledgment. This research was supported by the National Science Council of the Republic of China (NSC 93-2113-M-006-010).

References and Notes

- (1) Kasturirangan, H.; Ramakrishnan V.; Kuriacose, J. C. *J. Catal.* **1981**, *69*, 216–217.
- (2) Pavlik, J. W.; Tantayanon, S. *J. Am. Chem. Soc.* **1981**, *103*, 6755–6757.
- (3) Fox, M. A.; Chen, M.-J. *J. Am. Chem. Soc.* **1983**, *105*, 4497–4499.
- (4) Nishimoto, S.; Ohtani, B.; Yoshikawa, T.; Kagiya, T. *J. Am. Chem. Soc.* **1983**, *105*, 7180–7182.
- (5) Yanagida, S.; Kizumoto, H.; Ishimaru, Y.; Pac, C.; Sakurai, H. *Chem. Lett.* **1985**, 141–144.
- (6) Fox, M. A.; Younathan, J. N. *Tetrahedron* **1986**, *42*, 6285–6291.
- (7) Prinet, M.; Pichat, P.; Mathieu, M.-V. *J. Phys. Chem.* **1971**, *75*, 1221–1226.
- (8) Boccuzzi, F.; Guglielminotti, E. *Sens. Actuators, B* **1994**, *21*, 27–31.
- (9) Basu, P.; Ballinger, T. H.; Yates, J. T., Jr. *Rev. Sci. Instrum.* **1988**, *59*, 1321–1327.
- (10) Wong, J. C. S.; Linsebigler, A.; Lu, G.; Fan, J.; Yates, J. T., Jr. *J. Phys. Chem.* **1995**, *99*, 335–344.
- (11) Suda, Y.; Morimoto, T.; Nagao, M. *Langmuir* **1987**, *3*, 99–104.
- (12) Calvert, J. G.; Pitts, J. N., Jr. *Photochemistry*; John Wiley and Sons: New York, 1966.
- (13) Mckean, D. C.; Ellis, I. A. *J. Mol. Struct.* **1975**, *29*, 81–96.
- (14) Murphy, W. F.; Zerbetto, F.; Duncan, J. L.; Mckean, D. C. *J. Phys. Chem.* **1993**, *97*, 581–595.
- (15) Nunney, T. S.; Birtill, J. J.; Raval, R. *Surf. Sci.* **1999**, *427*, 282–287.
- (16) Erley, W.; Xu, R.; Hemminger, J. C. *Surf. Sci.* **1997**, *389*, 272–286.
- (17) Qin, D.; Chang, W.; Chen, Y.; Zhou, J.; Chen, Y.; Gong, M. *J. Catal.* **1993**, *142*, 719–724.
- (18) Naccache, C.; Meriaudeau, P.; Che, M.; Tenche, A. *J. Trans. Faraday Soc.* **1971**, *67*, 506–512.
- (19) Pan, J.-M.; Maschhoff, B. L.; Diebold, U.; Madey, T. E. *J. Vac. Sci. Technol. A* **1992**, *10*, 2470–2476.
- (20) Markovits, A.; Ahdjoudj, J.; Minot, C. *Surf. Sci.* **1996**, *365*, 649–661.
- (21) Ault, B. S.; Stelnback, E.; Pimental, G. C. *J. Phys. Chem.* **1975**, *79*, 615–620.
- (22) Andrews, L.; Davis, S. R.; Johnson, G. L. *J. Phys. Chem.* **1986**, *90*, 4273–4282.
- (23) Bevitt, J.; Chapman, K.; Crittenden, D.; Jordan, M. J. T. *J. Phys. Chem. A* **2001**, *105*, 3371–3378.
- (24) Su, C.; Yeh, J.-C.; Chen, C.-C.; Lin, J.-C.; Lin, J.-L. *J. Catal.* **2000**, *194*, 45–54.
- (25) Wu, W.-C.; Chuang, C.-C.; Lin, J.-L. *J. Phys. Chem. B* **2000**, *104*, 8719–8724.
- (26) Colthup, N. B.; Daly L. H.; Wiberley, S. E. *Introduction to Infrared and Raman Spectroscopy*; Academic Press Inc.: San Diego, CA, 1990.
- (27) Liao, L.-F.; Lien, C.-F.; Shieh, D.-L.; Chen, M.-T.; Lin, J.-L. *J. Phys. Chem. B* **2002**, *106*, 11240–11245.
- (28) Wu, W.-C.; Liao, L.-F.; Chuang C.-C.; Lin, J.-L. *J. Catal.* **2000**, *195*, 416–419.
- (29) Hadjiivanov, K.; Bushev, V.; Kantcheva, M.; Klissurski, D. *Langmuir* **1994**, *10*, 464–471.
- (30) Nakamoto, K. *Infrared and Raman Spectra of Inorganic and Coordination Compounds*; John Wiley and Sons: New York, 1986.
- (31) Chuang, C.-C.; Wu, W.-C.; Lee, M.-X.; Lin, J.-L. *Phys. Chem. Chem. Phys.* **2000**, *2*, 3877–3882.
- (32) Zhuang, J.; Rusu, C. N.; Yates, J. T., Jr. *J. Phys. Chem. B* **1999**, *103*, 6957–6967.
- (33) Solymosi, F.; Bansagl, T. *J. Phys. Chem.* **1979**, *83*, 552.
- (34) Liao, L.-F.; Wu, W.-C.; Chen, C.-Y.; Lin, J.-L. *J. Phys. Chem. B* **2001**, *105*, 7678–7685.
- (35) Busca, G.; Lamotte, J.; Lavalley J.-C.; Lorenzelli, V. *J. Am. Chem. Soc.* **1987**, *109*, 5197–5202.
- (36) Spinner, E.; Rowe, J. E. *Aust. J. Chem.* **1979**, *32*, 481–501.
- (37) Ishibashi, K.; Fujishima, A.; Watanabe, T.; Hashimoto, K. *J. Phys. Chem. B* **2000**, *104*, 4934–4938.
- (38) Ramis, G.; Busca, G.; Lorenzelli, V.; Forzatti, P. *Appl. Catal.* **1990**, *64*, 243–257.
- (39) Chuang, C.-C.; Shiu J.-S.; Lin, J.-L. *Phys. Chem. Chem. Phys.* **2000**, *2*, 2629–2633.
- (40) Haugen, C. M.; Whitten, D. G. *J. Am. Chem. Soc.* **1989**, *111*, 7281–7282.
- (41) Low, G. K.-C.; McEvoy, S. R.; Matthews, R. W. *Environ. Sci. Technol.* **1991**, *25*, 460.
- (42) Barnes, K. K.; Mann, C. K. *J. Org. Chem.* **1967**, *32*, 1474.
- (43) Lien, C.-F.; Lin, Y.-F.; Lin, Y.-S.; Chen, M. T.; Lin, J.-L. *J. Phys. Chem. B* **2004**, *108*, 18261.